• Basic Research •

All-trans retinoic acid increases ARPE-19 cell apoptosis *via* activation of reactive oxygen species and endoplasmic reticulum stress pathways

Juan Wu[1], *Zhen-Ya Gao*[2], *Dong-Mei Cui*[1], *Hong-Hui Li*[3], *Jun-Wen Zeng*[1]

[1]State Key Laboratory of Ophthalmology, Zhongshan Ophthalmic Center, Sun Yat-sen University, Guangzhou 510060, Guangdong Province, China
[2]Xuchang University, School of Medicine, Xuchang 461000, Henan Province, China
[3]Chengdu Aier Eye Hospital, Chengdu 610000, Sichuan Province, China
Correspondence to: Jun-Wen Zeng. State Key Laboratory of Ophthalmology, Zhongshan Ophthalmic Center, Sun Yat-sen University, Guangzhou 510060, Guangdong Province, China. zeng_zoc@163.com
Received: 2020-04-23 Accepted: 2020-06-02

Abstract

● **AIM:** To explore the apoptosis of ARPE-19 cells after the treatment with different doses of all-trans-retinoic acid (ATRA).

● **METHODS:** ARPE-19 cells were used in the *in-vitro* experiment. Flow cytometry assay was employed to evaluate the level of reactive oxygen species (ROS) and apoptosis. The effects of ATRA (concentrations from 2.5 to 20 μmol/L) on the expression of endoplasmic reticulum stress (ERS) markers *in vitro* were evaluated by Western blot and real-time quantitative polymerase chain reaction (qRT-PCR) assays. The contribution of ROS and ERS-induced apoptosis *in vitro* was determined by using N-acetyl-L-cysteine (NAC) and Salubrinal, an antagonist of NAC and ERS, respectively.

● **RESULTS:** Flow cytometry showed that ATRA significantly increased ARPE-19 cell apoptosis and ROS levels in each group (F=86.39, P<0.001; F=116.839, P<0.001). Western blot and qRT-PCR revealed that levels of CHOP and BIP were elevated in a concentration-dependent pattern after the cells were incubated with ATRA (2.5-20 μmol/L). The upregulation of VEGF-A and CHOP induced by ATRA could be inhibited by NAC (antioxidant) and Salubrinal (ERS inhibitor) *in vitro*.

● **CONCLUSION:** ATRA induces the apoptosis of ARPE-19 cells *via* activated ROS and ERS signaling pathways.

● **KEYWORDS:** all-trans-retinoic acid; retinal pigment epithelium; apoptosis; reactive oxygen species; endoplasmic reticulum stress

DOI:10.18240/ijo.2020.09.01

Citation: Wu J, Gao ZY, Cui DM, Li HH, Zeng JW. All-trans retinoic acid increases ARPE-19 cell apoptosis *via* activation of reactive oxygen species and endoplasmic reticulum stress pathways. *Int J Ophthalmol* 2020;13(9):1345-1350

INTRODUCTION

In age-related macular degeneration (AMD), certain kinds of neurons undergo cellular apoptosis in macula, resulting in blindness and irreversible sight loss. Early events in AMD mainly include the progressive degeneration and apoptosis of the retinal pigment epithelium (RPE), which is a single layer of retinal pigment cells nourishing retina[1-3]. The phagocytosis function, anatomic location and high metabolic activity make RPE easy to be damaged during multiple injuries[4]. It is widely known that RPE cell apoptosis contributed to the development of AMD. Among all the factors promoting apoptosis, oxidative stress plays a pivotal role.

Retinoid cycle, commonly known as visual cycle, is essential in the retina of the vertebrates[5]. As all-trans-retinoic acid (ATRA), a strong photosensitizer bearing aldehyde, can result in cell death[6-8]. When the retina is exposed to light, ATRA can be synthesized from 11-cis-retinal. ATRA in RPE and photoreceptor cells plays a vital role in the visual cycle.

Excessive ATRA in RPE cells can contribute to cell apoptosis[9-10] which leads to degeneration diseases in retina. Reactive oxygen species (ROS) levels, as a key factor in RPE degeneration, could be elevated by ATRA *via* mediating the NAPDH oxidase[11]. In RPE cells, oxidative injuries can result in unfolded protein response (UPR) and endoplasmic reticulum stress (ERS)[12-13]. However, the underlying mechanisms of RPE degeneration induced by ATRA still remain unknown.

In this research, ROS production in ARPE-19 cells treated by ATRA was investigated. ERS was also evaluated. The associations between ATRA-induced ROS generation and ERS were elucidated. Our results revealed the toxicity of ATRA in ARPE-19 cells, and provided new understandings on AMD pathogenesis.

Table 1 The sequences of primers used in the real-time PCR

Gene	GenBank number	Sequence
CHOP	NM_001195057.1	Forward: 5'-CTCCCTTGGTCTTCCTCCTC-3'
		Reverse: 5'-CTTCTCTGGCTTGGCTGACT-3'
BIP	NM_005347.4	Forward: 5'-CACCTTGAACGGCAAGAACT-3'
		Reverse: 5'-AAGAACCAGCTCACCTCCAA-3'
GAPDH	NM_001256799.2	Forward: 5'-GGAGCGAGATCCCTCCAAAAT-3'
		Reverse: 5'-GGCTGTTGTCATACTTCTCATGG-3

CHOP: C/EBP homologous protein; BIP: Binding immunoglobulin protein; GAPDH: Glyceraldehyde-3-phosphate dehydrogenase; PCR: Polymerose chain reaction.

MATERIALS AND METHODS

Cell Culture and Treatment ARPE-19 cells were cultured by using Dulbecco's modified Eagle medium/Ham's Nutrient Mixture F12 (1:1; DMEM/F12, Gibco, Grand Island, NY, USA) added with penicillin (100 IU/mL), streptomycin (Invitrogen, Carlsbad, CA, USA), and fetal bovine serum (10%; FBS, Gibco, Australia) in a 37℃ humidified incubator with CO_2 (5%). To prepare for Western blot, real-time polymerase chain reaction (PCR) and immunofluorescence assay, 100-mm^2 dishes (Corning), 60-mm^2 dishes (Corning) and 6-well plates (Corning) were used to culture cells, respectively.

Dimethyl sulfoxide (DMSO, Sigma-Aldrich, USA) was used to dissolve ATRA (Sigma-Aldrich, USA) and the concentration for stock was 10 μmol/L. DMEM/F12 was used to dilute ATRA before use. ATRA was stored in the -20℃ refrigerator without light.

Cell Counting Kit-8 Assay Cells were cultured in 96-well plates with 5000 cells in each well. Various concentrations of ATRA (0, 2, 4, 6, 8, 10, 12, 14, 16, 18, and 20 μmol/L; 10 μL) were used to treat the cells after the cells were preincubated with DMEM/F12 +0.1% FBS for 24h. The wells only added with culture medium were set as the blank control group. After culture for 24 or 48h, 10 μL cell counting kit-8 (CCK-8; Dojindo, Kumamoto, Japan) was diluted with 100 μL DMEM/F12 and the mixture was added into the cells. After incubation for 1-4h, the absorbance was detected at 450 nm by using a microplate reader (PowerWave XS Microplate Spectrophotometer, Bio-Tek, USA). Independent experiments were repeated for five times at least.

Apoptosis Assay by Using Flow Cytometry Annexin V-fluorescein isothiocyanate apoptosis detection kit (Becton-Dickinson, CA, USA) was applied to apoptosis assay. After treated by ATRA, the mixture of propidium iodide (PI), annexin V-fluorescein isothiocyanate annexin and 1×binding buffer was used to suspend the cells. FACS scan flow cytometer machine (Becton-Dickinson San Jose, CA, USA) was employed to measure the fluorescence.

Flow Cytometric Analysis of Reactive Oxygen Species Total ROS was determined by dichloro-dihydro-fluorescein diacetate (DCFH-DA) staining assay (Merck Millipore, DE, USA). ARPE-19 cells were treated with a series of concentrations (20, 15, 10, 5, and 0 μmol/L) of ATRA. Then, 1 μmol/L ROS and DCFH-DA, a fluorescent probe, were added into cells. After culture for 30min, FACS scan flow cytometry machine (Becton-Dickinson San Jose, CA, USA) was used to measure the fluorescence.

RNA Extraction, Complementary DNA Synthesis, and Quantitative Real-time Polymerase Chain Reaction TRIzol (Invitrogen Inc., Carlsbad, CA, USA) was applied to purify RNA, and ReverTra Ace quantitative real-time polymerase chain reaction (qRT-PCR) kit (TOYOBO, Japan) was used in the synthesis of complementary DNA (cDNA). Brilliant SYBR Green qRT-PCR Master Mix (TaKaRa, Japan) and CFX96 qRT-PCR detection system (Bio-Rad, USA) were used to perform qRT-PCR. The synthesized cDNA was amplified for 40 cycles and the annealing was performed at 60℃. The primer sequences (Sangon Biotech, Shanghai, China) used in qRT-PCR are shown in Table 1. The efficiencies of primer pairs' amplification had been validated. The CT value of the negative control (without cDNA) was greater than 33. At least 3 different samples were used in every qRT-PCR assay. To determine the levels of the target genes, $2^{-\Delta\Delta ct}$ method was applied. GAPDH was set as the internal reference.

Western Blot Analysis After treated with ATRA (20, 10, 15, 5, 2.5, and 0 μmol/L) for 24h and 48h, the cells were collected. Electrophoresis was conducted after cell lysis by using RIPA lysis buffer (Beyotime, Haimen, China). The polyvinylidene fluoride (PVDF) membranes (Millipore, Bedford, MA, USA) were used in protein transfer. The membranes then were incubated with 5% nonfat milk in room temperature for one hour. Afterwards, the membranes were incubated with the primary antibodies, including binding immunoglobulin protein (BIP; 1:1000, #3177, Cell Signaling Technology, USA), C/EBP homologous protein (CHOP; 1:1000, #2895, Cell Signaling Technology, USA), anti-VEGF-A (1:1000, #ab46154, abcam, USA). The protein bands were visualized using horseradish peroxidase (HRP)-conjugated secondary antibodies and

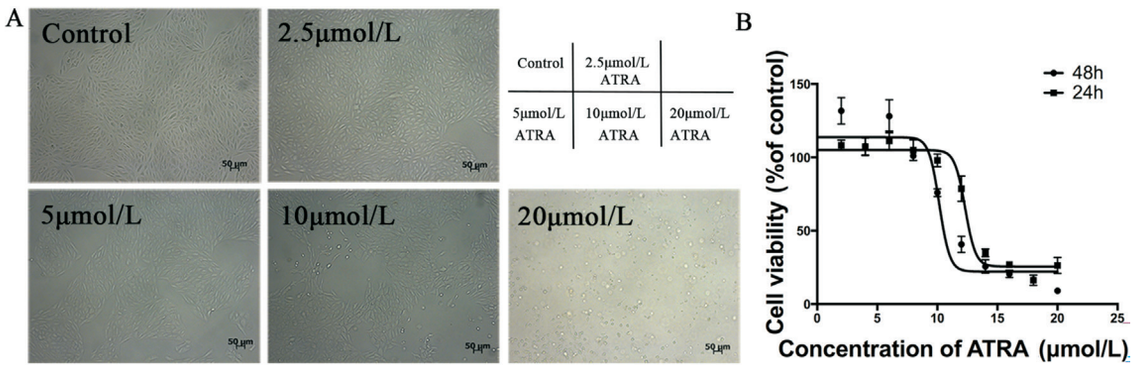

Figure 1 The influence of ATRA on cell viability A: The cell morphology at different concentrations of ATRA. B: Following treatment for 24h and 48h, CCK-8 assay assesses the survival of cell treated with ATRA at different concentration from 0-20 μmol/L. The results from 3 independent experiments are presented as average value±SEM.

Enhanced Chemiluminescence (ECL) Western blotting detection system (Millipore, USA). Bio-Rad Quantity One Imaging software (Bio-Rad, USA) was used in the analysis.

Confocal Laser Microscopy ARPE-19 cells were induced by ATRA and seeded on coverslips. After the cells were rinsed with PBS three times, 4% paraformaldehyde was applied to fix the cells for 15min. Afterwards, the mixture of 1% bovine serum albumin (BSA), 0.1% Triton X-100 and PBS was incubated with the coverslips for 30min. Subsequently, primary antibodies were used for incubation with the cells at room temperature for 2h. The antibodies included BIP (1:400, #3177, Cell Signaling Technology), and CHOP (1:200, #2895, Cell Signaling Technology). After the cells were washed by PBS, secondary antibodies (1:400, Cell Signaling Technology) were used for incubation. Afterwards, 2-(4-amidinophenyl)-6-indolecarbamidine dihydrochloride (DAPI; 5 mg/mL) was added to stain the nuclei. Anti-fade mounting medium was used for mounting. Zeiss Confocal Spectral Microscope (Carl Zeiss, Jena, Germany) was applied to obtain images.

Statistical Analysis SPSS 22.0 was applied in statistical analysis. Graphpad prism 7 was used for mapping. The results were presented as average value ±SD. Bonferroni's multiple comparison test and one-way analysis of variance (ANOVA) were applied to evaluate whether the inter-group differences were statistically significant. If *P* value were less than 0.05, the difference was considered to be statistically significant.

RESULTS

Influence of ATRA on Cell Viability Various concentrations of ATRA (2.5-20 μmol/L) were used treat ARPE-19 cells to assess whether ATRA could influence the cell viability. When ATRA concentrations were between 2.5 and 10 μmol/L, the apoptosis level was low (<10%) and the morphology of the cell was normal. When the concentrations were between 10 and 20 μmol/L (Figure 1A), the cells began to shrink. The results of CCK-8 assay showed that ATRA promoted cell growth when the concentrations were between 2 and 6 μmol/L, but significantly inhibited cell growth when concentrations were between 10 and 20 μmol/L. Cell viability dropped below 30% after treatment with 20 μmol/L ATRA (Figure 1B). After treatment for 24h and 48h, ATRA exhibited dose-dependent effects on cell survival, with low doses increasing survival and high doses inhibiting survival. The half maximal inhibitory concentrations (IC_{50}) of ATRA following treatment for 24h and 48h were 13.88 μmol/L and 11.99 μmol/L, respectively.

Flow Cytometry Analysis of Apoptosis and ROS Levels After treatment with 2.5 and 5 μmol/L ATRA for 24h, cell apoptosis decreased compared with the control group (P<0.05). However, following treatment with 10, 15 and 20 μmol/L ATRA for 24h, the cell apoptosis rate increased when the concentration increased (P<0.001; Figure 2A, 2C). The generation of ROS was dramatically increased in comparison with the cells without treatment (P<0.001; Figure 2B, 2D). In the present study, when the concentration of ATRA was higher than 10 μmol/L, cell apoptosis was significantly increased. Thus, 10 μmol/L of ATRA was used as the test concentration in the confocal laser microscopy.

Endoplasmic Reticulum Stress in the Cells Treated by All-trans-retinoic Acid In this study, CHOP and BIP antibodies were used in Western blot. ARPE-19 cells were exposed to various concentrations of ATRA for 24h (Figure 3A). The images from confocal laser microscopy suggested that ATRA induced the generation of CHOP (Figure 3B) and BIP (Figure 3C). The Western blot analysis showed that expressions of CHOP (Figure 3D) and BIP (Figure 3F) were upregulated in response to increased concentrations of ATRA. The mRNA expression of CHOP (Figure 3E) and BIP (Figure 3G) was also elevated after incubation with increasing concentrations of ATRA.

Protective Effects of NAC and Salubrinal In the ARPE-19 cells treated by ATRA, previous research proved that there might be interactions among VEGF-A, CHOP, ROS and ERS. We further explored if the levels of VEGF-A and CHOP could

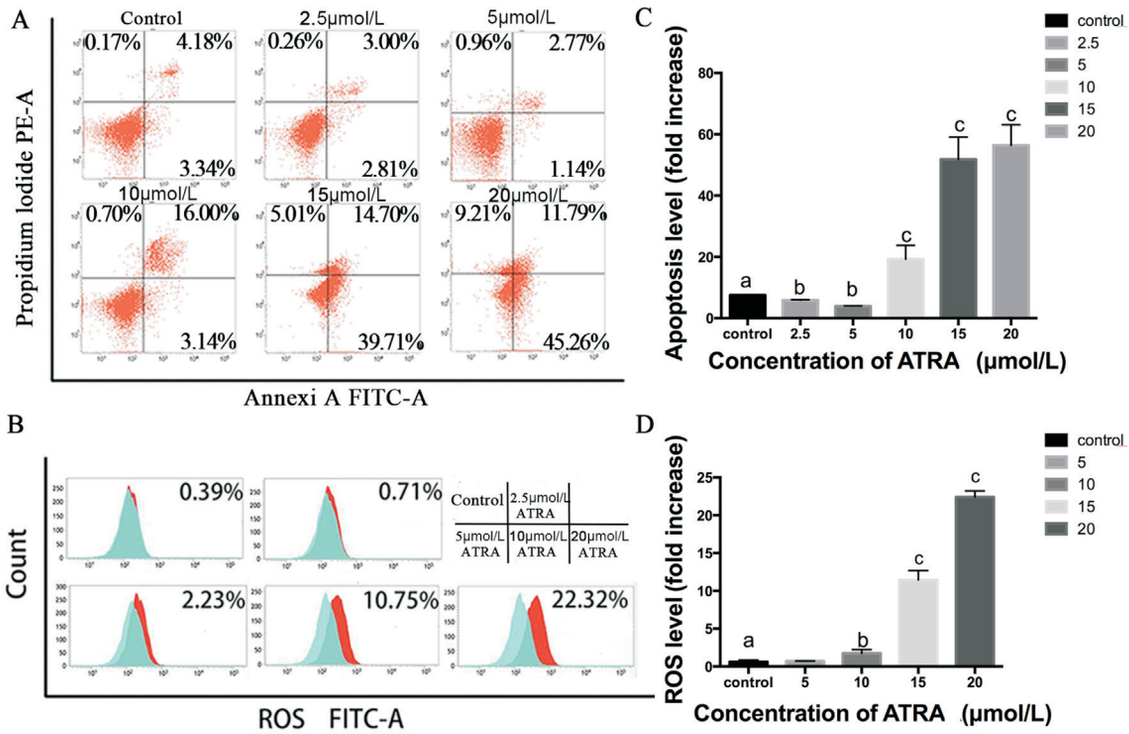

Figure 2 Flow cytometry analysis apoptosis and ROS levels A: After 24h treatment with ATRA (0-20 μmol/L), apoptosis was detected. The ration of apoptotic cells was calculated according to the results of flow cytometry. B: After ATRA treatment (0-20 μmol/L) for 24h, the ROS level was determined by using flow cytometry assay. C, D: Results were shown as the fold increase of fluorescence in the treatment group in comparison with the cells without treatment. The results from 3 independent experiments were shown as average value ±SEM. [a]Control group; [b]$P<0.05$; [c]$P<0.001$.

be inhibited by the antioxidant NAC and Salubrinal, an ERS inhibitor. As an antioxidant, NAC can clear free radicals and the working concentration is 5 mmol/L without cytotoxicity in this experiment. Salubrinal is an agent inhibiting ERS and can save cells from apoptosis induced by tunicamycin *via* suppressing the dephosphorylation of eIF2α, and the working concentration is 40 μmol/l without cytotoxicity. Thus, five groups were set, namely, control group, ATRA-treated group, ATRA-NAC group, ATRA-Salubrinal group and ATRA-NAC-Salubrinal group. After treatment for 24h, Western blot was conducted (Figure 4A). In comparison with the control group, ATRA could significantly increase the expression of CHOP and VEGF-A, while the upregulation of CHOP and VEGF-A induced by ATRA was inhibited in ATRA-NAC, ATRA-Salubrinal and ATRA-NAC-Salubrinal groups (Figure 4B, 4C).

DISCUSSION

ATRA and 11-cis-retinal have a pivotal role in vision. Free ATRA serves as an intermediate in the normal visual cycle[14]. Excessive ATRA can contribute to critical retinal disorders and the accumulation of products derived from retina in RPE[6], which may induce vision loss.

In our research, it was proved that excessive ATRA could cause injuries to RPE cells (Figure 1A). After ATRA (over 10 μmol/L) exposure, ROS production was dramatically raised compared with the control group (Figure 2B) and severe loss of RPE cells was observed (Figure 1B). ATRA is an endogenous substance in retina, which could be eliminated under normal conditions, and the lysosomes in RPE cells could trap the products derived from retina[8,15]. Free ATRA can be cleared by RPE and photoreceptor cells, but RPE cells may be injured when the concentrations of ATRA reached the threshold that RPE cells can tolerate (Figure 2A). In our experiments, RPE cells were treated with ATRA to establish an *in-vitro* model mimicking the conditions in which RPE cells were exposed to intensive and acute light or excessive accumulation of ATRA[16].

Previous research demonstrated that ATRA directly exerted poisonous effects on mitochondria *via* inhibiting the oxidation process in mitochondria or uncoupling oxidative phosphorylation when ATRA concentration was beyond a certain value[10]. Moreover, ATRA was able to increase the permeability of mitochondrial membrane, leading to the loss of essential enzymes and thus contributing to mitochondria damage. Additionally, excessive production of ROS in the cytoplasm induced by ATRA directly injured organelles and resulted in critical cellular injuries. ROS could also directly cause damage to the endoplasmic reticulum (ER).

ERS is considered to be a main factor contributing to AMD[17]. In retinal degeneration, risk factors of AMD including metabolic, oxidative and proteotoxic stress could induce ERS and UPR[18]. The main functions of UPR are ensuring regular

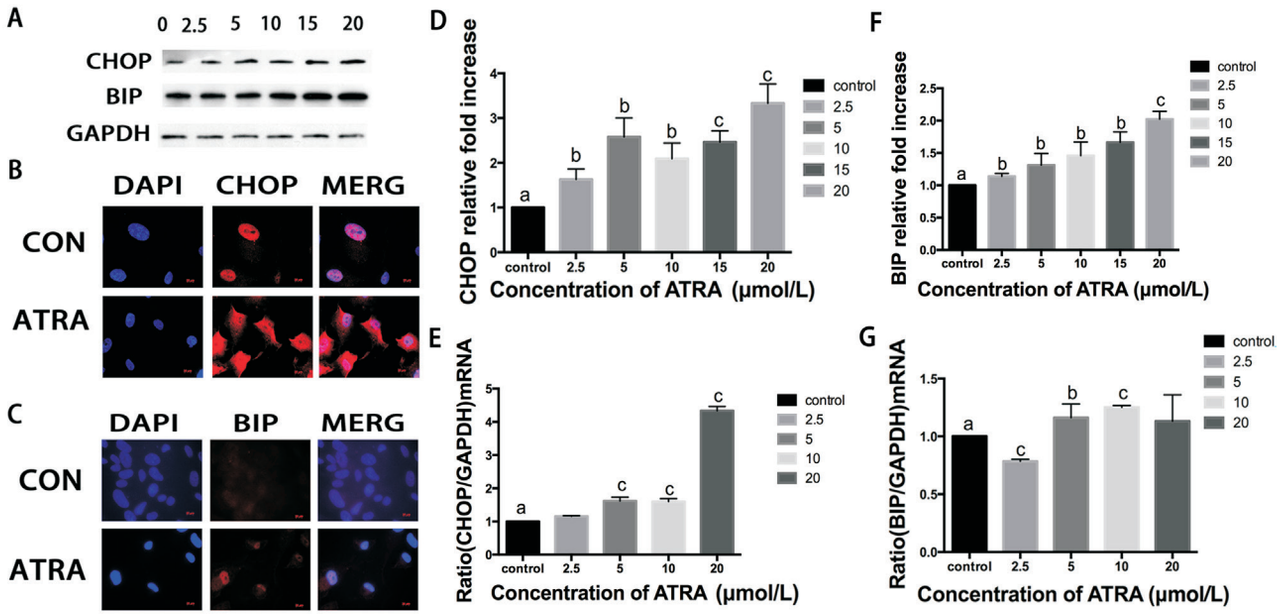

Figure 3 Activation of ERS in ATRA-treated ARPE-19 cells ARPE-19 cells were treated with various concentrations of ATRA for 24h. CHOP and BIP antibodies were used in Western blot (A). The levels of CHOP and BIP were raised after ATRA treatment (D, F), immunofluorescence confirmed the expression of CHOP and BIP (B, C). The mRNA expressions of CHOP (E) and BIP(G) were increased after cells were treated with increasing concentrations of ATRA. The results from 3 independent experiments were shown as average value ±SEM. [a]Control group; [b]P<0.05; [c]P<0.001. Immunofluorescence was applied to show the location of the expressed CHOP (red) and BIP (red). Nuclei were stained by DAPI (blue). Scale bar=50 μm.

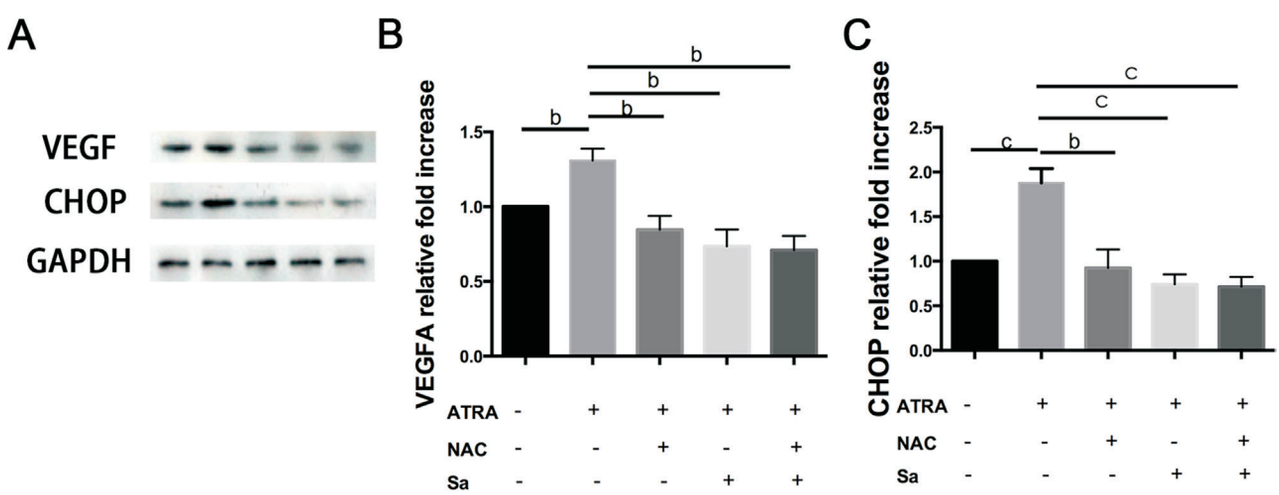

Figure 4 NAC and Salubrinal inhibited the expression of VEGF-A and CHOP A-C: Cell lysates were obtained after treatment with 10 μmol/L ATRA with or without 5 mmol/L NAC or 40 μmol/L Salubrinal for 24h. Western blot was conducted using VEGF-A (B) and CHOP (C) antibodies. Three independent experiments were performed and the results were shown as average value±SEM .[b]P<0.05, [c]P<0.001.

function of ER and reducing the environmental damages to cells[19], and BIP played an important role in regulating ERS-related pathways[20-21]. Unfolded and misfolded proteins can trigger the expression of BIP[22] and finally be cleared by this ER chaperone[23]. In this research, the BIP expression level was raised after ATRA treatment. With regard to the signaling pathways of the UPR, three pathways (PERK, IRE1α, and ATF6) initiated by sensors of ERS have attracted the most attention in terms of the cellular ERS response[24]. CHOP promotes apoptosis in ERS and is the main target of ATF4 transcription factor[25]. It was previously demonstrated that CHOP participated in regulating the expression of Ero1α in ERS, which could increase ROS production in ER[26]. In this present research, ATRA could increase the expression of CHOP *in vitro*, which could be ameliorated by NAC pretreatment. Our results implied that NAC could ameliorate the apoptosis induced by ERS *via* downregulating CHOP levels (Figure 4C). Furthermore, the VEGF-A (a marker for neovascularization) expression level was elevated after ATRA treatment. VEGF-A can affect the cells in choriocapillaris and is related to

subretinal neovascularization in AMD[27]. VEGF activation is closely relayed with ROS production, which increases the expressions of the genes with protective functions *via* the antioxidant response element enhancer[2]. Similarly, in our study, Salubrinal attenuated the increase of VEGF-A expression induced by ATRA (Figure 4B), which implied that ROS could interact with ERS.

In conclusion, excessive accumulation of ATRA would lead to ROS and ERS generation in ARPE-19 cells, which contributed to the development of AMD. Hence, reducing ATRA levels might be a strategy to treat AMD. Since ATRA could exert cytotoxic effects and result in oxidative stress, inhibiting retinoic metabolism pathways could be a new therapy in treating AMD.

ACKNOWLEDGEMENTS

Foundation: Supported by National Natural Science Foundation of China (No.81170872).

Conflicts of Interest: Wu J, None; **Gao ZY,** None; **Cui DM,** None; **Li HH,** None; **Zeng JW,** None.

REFERENCES

1 Zarbin M, Sugino I, Townes-Anderson E. Concise review: update on retinal pigment epithelium transplantation for age-related macular degeneration. *Stem Cells Transl Med* 2019;8(5):466-477.

2 del Priore LV, Kuo YH, Tezel TH. Age-related changes in human RPE cell density and apoptosis proportion *in situ*. *Invest Ophthalmol Vis Sci* 2002;43(10):3312-3318.

3 He S, Yaung J, Kim YH, Barron E, Ryan SJ, Hinton DR. Endoplasmic reticulum stress induced by oxidative stress in retinal pigment epithelial cells. *Graefes Arch Clin Exp Ophthalmol* 2008;246(5):677-683.

4 Ao J, Wood JP, Chidlow G, Gillies MC, Casson RJ. Retinal pigment epithelium in the pathogenesis of age-related macular degeneration and photobiomodulation as a potential therapy? *Clin Exp Ophthalmol* 2018;46(6):670-686.

5 Saari JC. Vitamin A and vision. *Subcell Biochem* 2016;81:231-259.

6 Maeda A, Maeda T, Golczak M, Palczewski K. Retinopathy in mice induced by disrupted all-trans-retinal clearance. *J Biol Chem* 2008;283(39):26684-26693.

7 Masutomi K, Chen CH, Nakatani K, Koutalos Y. All-trans retinal mediates light-induced oxidation in single living rod photoreceptors. *Photochem Photobiol* 2012;88(6):1356-1361.

8 Sparrow JR, Wu Y, Kim CY, Zhou J. Phospholipid meets all-trans-retinal: the making of RPE bisretinoids. *J Lipid Res* 2010; 51(2):247-261.

9 Li J, Cai XH, Xia QQ, Yao K, Chen JM, Zhang YL, Naranmandura H, Liu X, Wu YL. Involvement of endoplasmic reticulum stress in all-trans-retinal-induced retinal pigment epithelium degeneration. *Toxicol Sci* 2015;143(1):196-208.

10 Hussain RM, Gregori NZ, Ciulla TA, Lam BL. Pharmacotherapy of retinal disease with visual cycle modulators. *Expert Opin Pharmacother* 2018;19(5):471-481.

11 Minasyan L, Sreekumar PG, Hinton DR, Kannan R. Protective mechanisms of the mitochondrial-derived peptide humanin in oxidative and endoplasmic reticulum stress in RPE cells. *Oxid Med Cell Longev* 2017;2017:1675230.

12 Tangvarasittichai O, Tangvarasittichai S. Oxidative stress, ocular disease and diabetes retinopathy. *Curr Pharm Des* 2018;24(40): 4726-4741.

13 Sreekumar PG, Hinton DR, Kannan R. Endoplasmic reticulum-mitochondrial crosstalk: a novel role for the mitochondrial peptide humanin. *Neural Regen Res* 2017;12(1):35-38.

14 Sawada O, Perusek L, Kohno H, Howell SJ, Maeda A, Matsuyama S, Maeda T. All-trans-retinal induces Bax activation *via* DNA damage to mediate retinal cell apoptosis. *Exp Eye Res* 2014;123:27-36.

15 Parker RO, Crouch RK. Retinol dehydrogenases (RDHs) in the visual cycle. *Exp Eye Res* 2010;91(6):788-792.

16 Maeda A, Maeda T, Golczak M, Chou S, Desai A, Hoppel CL, Matsuyama S, Palczewski K. Involvement of all-trans-retinal in acute light-induced retinopathy of mice. *J Biol Chem* 2009;284(22): 15173-15183.

17 Oakes SA, Papa FR. The role of endoplasmic reticulum stress in human pathology. *Annu Rev Pathol* 2015;10:173-194.

18 Ariyasu D, Yoshida H, Hasegawa Y. Endoplasmic reticulum (ER) stress and endocrine disorders. *Int J Mol Sci* 2017;18(2):382.

19 Cybulsky AV. Endoplasmic reticulum stress, the unfolded protein response and autophagy in kidney diseases. *Nat Rev Nephrol* 2017;13(11):681-696.

20 Ryoo HD. Long and short (timeframe) of endoplasmic reticulum stress-induced cell death. *FEBS J* 2016;283(20):3718-3722.

21 Pobre KFR, Poet GJ, Hendershot LM. The endoplasmic reticulum (ER) chaperone BiP is a master regulator of ER functions: getting by with a little help from ERdj friends. *J Biol Chem* 2019;294(6):2098-2108.

22 Hardy B, Raiter A. Peptide-binding heat shock protein GRP78 protects cardiomyocytes from hypoxia-induced apoptosis. *J Mol Med* 2010;88(11):1157-1167.

23 Leitman J, Barak B, Benyair R, Shenkman M, Ashery U, Hartl FU, Lederkremer GZ. ER stress-induced eIF2-alpha phosphorylation underlies sensitivity of striatal neurons to pathogenic huntingtin. *PLoS One* 2014;9(3):e90803.

24 Walter P, Ron D. The unfolded protein response: from stress pathway to homeostatic regulation. *Science* 2011;334(6059):1081-1086.

25 Ma Y, Brewer JW, Diehl JA, Hendershot LM. Two distinct stress signaling pathways converge upon the CHOP promoter during the mammalian unfolded protein response. *J Mol Biol* 2002;318(5):1351-1365.

26 Song B, Scheuner D, Ron D, Pennathur S, Kaufman RJ. Chop deletion reduces oxidative stress, improves beta cell function, and promotes cell survival in multiple mouse models of diabetes. *J Clin Invest* 2008;118(10):3378-3389.

27 Rating P, Freimuth MA, Stuschke M, Bornfeld N. Adjuvant radiotherapy during anti-VEGF in neovascular age-related macular degeneration. *Ophthalmologe* 2017;114(4):370-374.